

Uncertainty quantification of an empirical shell-model interaction using principal component analysis

Jordan M. R. Fox* and Calvin W. Johnson†

San Diego State University, San Diego, California, USA

(Dated: May 5, 2022)

Abstract

Recent investigations have emphasized the importance of uncertainty quantification (UQ) to describe errors in nuclear theory. We carry out UQ for configuration-interaction shell model calculations in the $1s-0d$ valence space, investigating the sensitivity of observables to perturbations in the 66 parameters (matrix elements) of a high-quality empirical interaction. The large parameter space makes computing the corresponding Hessian numerically costly, so we construct a cost-effective approximation using the Feynman-Hellmann theorem. Diagonalizing the approximated Hessian yields the principal components: linear combinations of parameters ordered by sensitivity. This approximately decoupled distribution of parameters facilitates theoretical error propagation onto structure observables: electromagnetic transitions, Gamow-Teller decays, and dark-matter interaction matrix elements.

* jfox@sdsu.edu

† cjohnson@sdsu.edu

I. INTRODUCTION

Few if any theories are free from limitations, errors, and uncertainties. In growing recognition of this truism, recent advancements in nuclear structure theory have emphasized the importance of theoretical uncertainty quantification (UQ) [1–6]. Two approaches for theoretical UQ are *sensitivity analysis*, which determines uncertainty in highly parameterized models [7], and *perturbative analysis*, where an underlying effective theory allows one to estimate, at any given order, the error from leaving out the next order [8, 9].

One of the fundamental frameworks of nuclear structure, the configuration-interaction shell model [10, 11], can be approximately divided into empirical or phenomenological [10, 12] and *ab initio* methodologies, such as the no-core shell model [13, 14]. Given that for the former, individual matrix elements in the lab frame (single-particle coordinates) are fitted, while the latter is typically built upon chiral effective field theory, it’s not surprising that sensitivity analysis has been applied to empirical calculations [7] and perturbative analysis to *ab initio* calculations [8, 15]. Here we do not consider related but distinct methodologies such as coupled clusters [16]. We note but do not comment further on efforts to construction interactions that ‘look like’ traditional empirical calculations but are derived with significant rigor from *ab initio* forces [17].

While no-core shell model is arguably more rigorous than empirical light nuclei, that is, approximately mass number $A < 16$. Empirical shell-model calculations have a long, rich, and successful history, and, importantly, have been applied to a wide range of nuclei far beyond the $0p$ shell, but the theoretical underpinnings are more heuristic.

Following previous work in the $0p$ -shell [7], we carry out a sensitivity analysis on an widely-used, ‘gold standard’ empirical interaction, Brown and Richter’s universal *sd*-shell interaction, version B, or USDB [18]. Here, ‘*sd*-shell’ means the valence space is limited to $1s$ and $0d$ single-particle orbits, with an inert ^{16}O core.

In fitting their interaction, Brown and Richter followed a standard procedure [10]. They minimized the reduced χ^2 , which serves as the *objective function*, by taking the first derivatives of χ_{red}^2 with respect to the parameters, which yield the linear response of calculated energies to perturbations of the parameters, and then carried out gradient descent on the sixty-six

independent parameters, here 63 two-body matrix elements and three single-particle energies. In the fit they found that about five or six linear combinations of parameters were the most important. (Interesting, a similar result was found for random values of the matrix elements [19]).

For a full sensitivity analysis, one must characterize the objective function. In Laplace's approximation (see III.A), one assumes the objective function, here χ_{red}^2 , is well approximated by a Gaussian. Even so, the matrix of second derivatives, or the *Hessian*, needed to fully describe such a Gaussian are quite demanding to obtain.

We therefore we rely upon a further simplification, approximating the Hessian by the same linear response (first derivatives of the energies), which are efficiently computed by the Feynman-Hellmann theorem [20, 21]. As discussed below, this principal component analysis of the sensitivity is, in this approximation, singular value decomposition of the linear response. Although this approximation needs further investigation, our initial work suggests this is indeed a good approximation.

II. THE EMPIRICAL CONFIGURATION-INTERACTION SHELL MODEL

Configuration-interaction many-body methods expand the wave function in a basis $\{|a\rangle\}$, usually orthonormal,

$$|\psi_\alpha\rangle = \sum_a c_{\alpha,a} |a\rangle. \quad (1)$$

For the basis we use the occupation representation of Slater determinants, that is, antisymmetrized products of single-particle states. We furthermore uses basis states with fixed total J_z , also called an M -scheme basis. The Hamiltonian is then formally represented in second quantization,

$$\hat{\mathcal{H}} = \sum_{r,s} T_{rs} \hat{a}_r^\dagger \hat{a}_s + \frac{1}{4} \sum_{rstu} V_{rs,tu} \hat{a}_r^\dagger \hat{a}_s^\dagger \hat{a}_u \hat{a}_t, \quad (2)$$

where typically one takes T_{rs} as diagonal *single-particle energies*, and the $V_{rs,tu}$ are two-body matrix elements, always coupled up to an angular momentum scalar so that angular momentum J is a good quantum number of eigenstates. The simplicity of the M scheme

allows for very fast calculation [22, 23] of the matrix elements

$$\mathcal{H}_{a,b} = \langle a | \hat{\mathcal{H}} | b \rangle,$$

which leads to large but sparse matrices, ripe for the Lanczos algorithm [24] to extract extremal eigenpairs,

$$\hat{\mathcal{H}}|\psi_\alpha\rangle = E_\alpha|\psi_\alpha\rangle. \quad (3)$$

See [10–12] for a multitude of important and interesting details.

We assume a frozen ^{16}O core and use the $1s-0d$ single-particle valence space, also called the sd -shell. Assuming both angular momentum J and isospin T are good quantum numbers, one has only three independent single-particle energies and 63 independent two-body matrix element, for a total of 66 parameters. Because each of those parameters appears linearly in the Hamiltonian, we can write

$$\hat{\mathcal{H}} = \sum_i \lambda_i \hat{\mathcal{O}}_i \quad (4)$$

where $\hat{\mathcal{O}}_i$ is some dimensionless one- or two-body operator. Thus the parameters λ have dimensions of energy.

The set of parameters λ_i we used are Brown and Richter’s universal sd -shell interaction version B (USDB) [18], which, along with its sister interaction USDA, are the current “gold standards” for empirical sd -shell calculations. The present study seeks to extend this model by computing theoretical uncertainties on model parameters and shell-model observables [25, 26].

Experimental energies in this paper are the same used in the original fit of the USDB Hamiltonian: absolute energies, relative to the ^{16}O core and with Coulomb differences subtract, of 608 states in 77 nuclei with $A = 21 - 40$. The data excludes any experimental uncertainties greater than 200 keV, and most are smaller, on the order of 10 keV.

In the rest of this paper, we estimate the uncertainty in the USDB parameters and, from those errors, estimate errors in observables such as energies, probabilities for selected electromagnetic and weak transitions, and for a matrix element relevant to dark matter direct detection.

III. BAYESIAN SENSITIVITY ANALYSIS

To define uncertainty on the USDB parameters, we start with Bayes' theorem. Let D represent data and λ the parameters, then

$$P(\boldsymbol{\lambda}|D) = \frac{P(D|\boldsymbol{\lambda})P(\boldsymbol{\lambda})}{P(D)} \propto P(D|\boldsymbol{\lambda})P(\boldsymbol{\lambda}) \quad (5)$$

This theorem states that the distribution of model parameters given the experimental data (the *posterior* = $P(\boldsymbol{\lambda}|D)$) is proportional to the distribution of data (the *likelihood* = $P(D|\boldsymbol{\lambda})$) given the parameter set, multiplied by the *a priori* distribution of parameters (the *prior* = $P(\boldsymbol{\lambda})$). Bayesian analysis [27] demands that we put some thought into the choice of prior, and the typical choice here is a *non-informative* prior, which seeks to minimize the effects of prior knowledge on this distribution. In this case, the non-informative prior is a uniform one, so we take $P(\boldsymbol{\lambda}) = 1$ [28].

With the non-informative prior, Bayes' theorem reduces to:

$$P(\boldsymbol{\lambda}|D) \propto P(D|\boldsymbol{\lambda}) \quad (6)$$

The goal now is to evaluate this expression, and we can choose between two methods: Laplace's Approximation (LA), or Markov-Chain Monte Carlo (MCMC). Due to its simplicity, we choose LA, as did a prior shell model study [7]. While MCMC advantageously makes no assumption as to the form of $P(\boldsymbol{\lambda}|D)$, it typically converges slowly for posteriors which are steep around extrema, so the computational cost of LA is comparatively much less.

A. Laplace's Approximation

Laplace's approximation is in essence a second-order Taylor approximation in the log-posterior, and thus we assume normally distributed errors on energies. Our likelihood function takes the form:

$$P(D|\boldsymbol{\lambda}) = \exp \left[-\frac{1}{2}\chi^2(\boldsymbol{\lambda}) \right] \quad (7)$$

where χ^2 is the usual sum of squared residuals:

$$\chi^2(\boldsymbol{\lambda}) = \sum_{\alpha=1}^N \left(\frac{E_{\alpha}^{exp} - E_{\alpha}^{SM}(\boldsymbol{\lambda})}{\Delta E_{\alpha}} \right)^2 \quad (8)$$

E_α^{exp} is the experimental excitation energy given in the data set and $E_\alpha^{SM}(\boldsymbol{\lambda})$ is the shell model prediction for that energy using the parameters $\boldsymbol{\lambda}$. The total uncertainty on the residual ΔE_α is expressed as experimental uncertainty ΔE_α^{exp} and some *a priori* theoretical uncertainty ΔE^{th} added in quadrature:

$$\Delta E_\alpha^2 = (\Delta_\alpha E^{th})^2 + (\Delta E_\alpha^{exp})^2 \quad (9)$$

Here we introduce ΔE^{th} as an expected error on the shell-model predictions of the data. It is obtained by evaluating the reduced chi-squared statistic at the USDB parameters $\chi_\nu^2 = \chi^2(\boldsymbol{\lambda}_{USDB})/d.o.f.$, and tuning ΔE^{th} so that $\chi_\nu^2 = 1$, which gives us $\Delta E^{th} \approx 150$ keV. This tuning is performed because a chi-squared statistic of unity per degrees-of-freedom is statistically interpreted as consistency between model errors ($E_\alpha^{exp} - E_\alpha^{SM}$) and total uncertainty ΔE_α .

By Eq. 7, there exists a global maximum of this likelihood function, called the maximum likelihood estimator (MLE). The optimal point for the posterior is called the “maximum *a posteriori*” (MAP), and here we see that $\boldsymbol{\lambda}_{MAP} = \boldsymbol{\lambda}_{MLE}$, but of course this is only in the special case of uniform prior. In this work, the MAP is equal to the USDB parameters.

$$\boldsymbol{\lambda}_{MAP} = \underset{\boldsymbol{\lambda}}{\operatorname{argmax}} P(\boldsymbol{\lambda}|D) = \underset{\boldsymbol{\lambda}}{\operatorname{argmax}} P(D|\boldsymbol{\lambda})P(\boldsymbol{\lambda}) = \underset{\boldsymbol{\lambda}}{\operatorname{argmin}} \chi^2(\boldsymbol{\lambda}) = \boldsymbol{\lambda}_{USDB} \quad (10)$$

The virtue of LA is we can immediately write down a properly normalized Gaussian approximation of the posterior.

$$P(\boldsymbol{\lambda}|D) \approx \frac{|H|}{(2\pi)^{k/2}} \exp \left[-\frac{1}{2} \bar{\boldsymbol{\lambda}}^T H \bar{\boldsymbol{\lambda}} \right], \quad (11)$$

where $[\bar{\boldsymbol{\lambda}}]_i = \boldsymbol{\lambda}_i - [\boldsymbol{\lambda}_{MLE}]_i$, k is the dimension of the parameter space, and H denotes the Hessian of the log-posterior (for brevity we refer to this as “the Hessian”). Note that we denote the Hessian matrix as H , and the Hamiltonian operator as $\hat{\mathcal{H}}$. The Hessian is defined as minus the second-derivative (in $\boldsymbol{\lambda}$) of the log-likelihood about the MAP.

$$H = -\nabla\nabla \log P(\boldsymbol{\lambda}|D)|_{\boldsymbol{\lambda}=\boldsymbol{\lambda}_{MAP}} \quad (12)$$

Because of Eq. 6, we can introduce an arbitrary constant c , so $P(\boldsymbol{\lambda}|D) = cP(D|\boldsymbol{\lambda})$:

$$H = -\nabla\nabla \log P(\boldsymbol{v}|D) = -\nabla\nabla \log cP(D|\boldsymbol{v}) = 0 - \nabla\nabla \log P(D|\boldsymbol{\lambda}) = +\frac{1}{2} \nabla\nabla \chi^2(\boldsymbol{\lambda}), \quad (13)$$

so the elements of H become:

$$H_{ij} = \frac{1}{2} \frac{\partial^2 \chi^2(\boldsymbol{\lambda})}{\partial \lambda_i \partial \lambda_j} \quad (14)$$

We can simplify this expression to put it in terms of eigenenergies:

$$\frac{\partial^2 \chi^2(\boldsymbol{\lambda})}{\partial \lambda_i \partial \lambda_j} = \sum_{\alpha=1}^N \frac{2}{(\Delta E_\alpha)^2} \left[\frac{\partial E_\alpha^{SM}}{\partial \lambda_i} \frac{\partial E_\alpha^{SM}}{\partial \lambda_j} + (E_\alpha^{SM} - E_\alpha^{expt}) \frac{\partial^2 E_\alpha^{SM}(\boldsymbol{\lambda})}{\partial \lambda_i \partial \lambda_j} \right] \quad (15)$$

so

$$H_{ij} = \sum_{\alpha=1}^N \frac{1}{(\Delta E_\alpha)^2} \frac{\partial E_\alpha^{SM}(\boldsymbol{\lambda})}{\partial \lambda_i} \frac{\partial E_\alpha^{SM}(\boldsymbol{\lambda})}{\partial \lambda_j} + \sum_{\alpha=1}^N \frac{(E_\alpha^{SM}(\boldsymbol{\lambda}) - E_\alpha^{expt})}{(\Delta E_\alpha)^2} \frac{\partial^2 E_\alpha^{SM}(\boldsymbol{\lambda})}{\partial \lambda_i \partial \lambda_j} \quad (16)$$

The first term in this expression dominates, so we define the *approximate Hessian* A as follows.

$$H_{ij} \approx \sum_{\alpha=1}^N \frac{1}{(\Delta E_\alpha)^2} \frac{\partial E_\alpha^{SM}(\boldsymbol{\lambda})}{\partial \lambda_i} \frac{\partial E_\alpha^{SM}(\boldsymbol{\lambda})}{\partial \lambda_j} \equiv A_{ij} \quad (17)$$

This approximation is good if the cross-derivative is small, for example if the energies were exactly linear in the parameters, or if the residual is small (meaning the model is good). The second term contains the cross-derivative, and this is more challenging to calculate, especially considering the size of the parameter-space. In the following section, we propose methods to approximate this.

While a numerical calculation of the full Hessian is possible in principle, the computational requirement is significant. For the full parameter space, one must evaluate the chi-squared function 8,844 times, in total computing 5,377,152 eigen-energies. While this is possible with the current resources, it is certainly worth exploring other options. The following method is our attempt to minimize computational cost while still giving a decent approximation to the Hessian.

To compute the derivatives of the energies, in Eq.17, we use the Feynman-Hellmann theorem,

$$\frac{\partial E_\alpha^{SM}(\boldsymbol{\lambda})}{\partial \lambda_i} = \left\langle \psi_\alpha \left| \frac{d\hat{\mathcal{H}}}{d\lambda_i} \right| \psi_\alpha \right\rangle = \langle \psi | \hat{\mathcal{O}}_i | \psi \rangle, \quad (18)$$

where the Hamiltonian (4) is linear in λ_j . Thus, for the first derivatives in (17), we can simply evaluate expectation values of the individual 1- and 2-body operators. Note that in the linear-model approximation, A is equal to the full Hessian, because the cross-derivative is always zero.

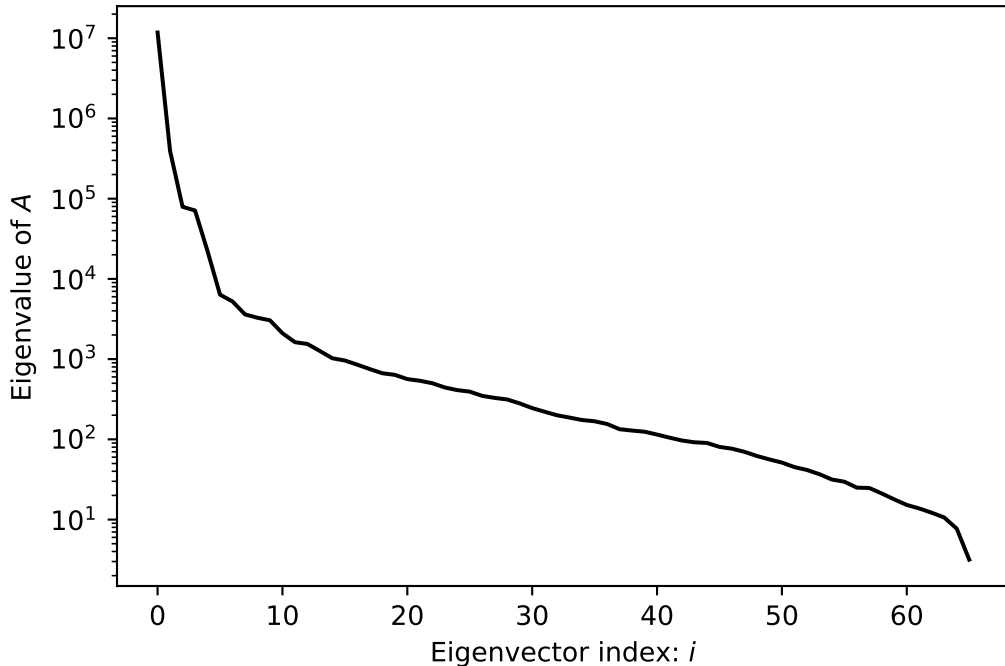


FIG. 1: Ordered eigenvalues of the approximate Hessian A , which equal the diagonal elements of D' . The eigenvalues are interpreted as the sensitivity of the corresponding linear combination or principal components of matrix elements (PCA-parameter). The first PCA-parameter carries 95% of the total sensitivity, and the first 5 PCA-parameters carry 99.6% of the sensitivity.

B. PCA Transformation

While errors introduced by approximating the Hessian ($H \rightarrow A$) are difficult to quantify numerically, we can still use A to gain new information. Diagonalizing the Hessian $UHU^T = D$, where D is diagonal, or its approximation

$$WAW^T = \Delta \quad (19)$$

where $\Delta \approx D$ is also diagonal, provides a transformation from the original parameters $\boldsymbol{\lambda}$ to new linear combinations of parameters,

$$\boldsymbol{\mu} = W^T \boldsymbol{\lambda}. \quad (20)$$

This is simply *principal component analysis* (PCA) of the Hessian, and so we call $\boldsymbol{\mu}$ the PCA parameters. In terms of our approximate Hessian, we can also understand this as a singular value decomposition (SVD) of the linear response $\partial E_\alpha/\partial\lambda_i$. Thus the eigenvalues found in Δ , and shown in Fig. 1, allow us to determine the most important linear combinations of parameters to the fit.

We can test the validity of the approximation $\Delta \approx D$ by numerically computing elements of WHW^T via finite difference (that is, elements of the full Hessian matrix in the PCA basis. Indeed, the off diagonals are nonzero, but small. We are carrying out further and systematic investigations. For the rest of this paper we will use the approximate Hessian (17). Furthermore, use the transformation from the original parameters $\boldsymbol{\lambda}$ to the PCA parameters $\boldsymbol{\mu}$.

IV. EVALUATING UNCERTAINTIES

The parameter covariance matrix is simply the inverse of the Hessian matrix, which we have approximated.

$$C(\boldsymbol{\lambda}) = H^{-1} \approx A^{-1} = W^T \Delta^{-1} W \quad (21)$$

The naive variance of the parameters is given by the diagonals of the covariance matrix, so that $\sigma(\lambda_i) = \sqrt{C_{ii}}$. This, however, ignores correlations between parameters and thus is an incomplete description of parameter errors. Better is to compute variances from the diagonalized Hessian matrix, and thus obtaining uncorrelated errors on the PCA parameters, $\sigma(\mu_i) = 1/\sqrt{D'_{ii}}$. These we give in Table I, and plot in Fig. 1. Here one sees the first few PCA parameters have very large sensitivity, and indeed the first 10 carry over 99.8% of the total; it is well-known lore in the nuclear shell-model community the fit of USDB and similar empirical interactions are dominated by only a few linear combinations, which here are the PCA parameters. Table I in fact demonstrates these parameters must be known to within a few keV or better; on the other hand 23 PCA parameters have uncertainties of 100-500 keV. At this point, it is important to remember that these variabilities are with respect to experimental data that only includes energies, so these low-variability PCA parameters could in principle be tuned to fit the interaction to various other observables without disrupting

| i | $[\Delta]_{ii}$ | σ_i (keV) |
|-----|-----------------|------------------|
| 1 | 11785561 | < 1 |
| 2 | 393793 | 2 |
| 3 | 79177 | 4 |
| 4 | 71236 | 4 |
| 5 | 22222 | 7 |
| 6 | 6357 | 13 |
| 7 | 5235 | 14 |
| 8 | 3612 | 17 |
| 9 | 3276 | 17 |
| 10 | 3049 | 18 |
| ... | ... | ... |
| 64 | 10.6 | 307 |
| 65 | 7.71 | 360 |
| 66 | 3.16 | 562 |

TABLE I: Statistics of linear-combinations of USDB matrix elements, or PCA parameters.

$[\Delta]_{ii}$ indicates eigenvalues of the approximate Hessian matrix A , which is interpreted as sensitivity of μ_i , and σ_i is the corresponding uncertainty. Thus the first PCA parameter is constrained to within 291 eV.

the fit to energies.

If the errors in the principal components u_i are independent, then the propagation of errors is straightforward. For any observable X ,

$$\sigma^2(X) = \sum_i \left(\frac{\partial X}{\partial \mu_i} \right)^2 \sigma^2(\mu_i) \quad (22)$$

Using (20),

$$\frac{\partial X}{\partial \mu_i} = \sum_j W_{ji} \frac{\partial X}{\partial \lambda_j} \quad (23)$$

and so

$$\sigma^2(X) = \sum_i \sigma^2(\mu_i) \sum_{jk} \frac{\partial X}{\partial \lambda_j} W_{ji} \frac{\partial X}{\partial \lambda_k} W_{ki} = \vec{g}^T C \vec{g} \quad (24)$$

where $g_i = \partial X / \partial \lambda_i$ is the linear response of any observable to perturbations in the original parameters. This is particularly useful in the case of energies, where we already have the linear response, thanks to the Feynman-Hellmann theorem.

For other observables, we do not use (24) directly. Instead, we generate perturbations in USDB by generating perturbations in the PCA parameters $\delta\boldsymbol{\mu}$ with a Gaussian distribution with width $\sigma(\mu_i)$ given by Table I. Because the errors are independent, or nearly so, in the PCA parameter representation, it is safe to generate the perturbations independently. We then transform back to the original representation of the matrix elements and read into a shell-model code [22, 23], find eigenpairs, and evaluate the reduced transition matrix element for one-body transition operators. Sampling 2,000 parameterizations gives sufficient convergence of the resulting set of matrix elements: assuming the transition strengths B_i are normally distributed with respect to small perturbations in the Hamiltonian, we take the theoretical uncertainty $\sigma(B_i)$ as equal to the standard deviation of the set of samples.

A. Results

For the energies used in the fit, we already have the elements of \vec{g} saved from computing the approximate Hessian, so this calculation is cheap. We can thus estimate covariance in the computed energies C_E by expanding this expression to a matrix equation.

$$C_E = B^T C_\lambda B \quad (25)$$

where $B_{i\alpha} = \partial E_\alpha / \partial \lambda_i$ is the linear response of the energies to perturbations in the parameters.

A few results for some of these estimated uncertainties are given in table II. Using these estimates, 75% of shell-model energies are within 1σ of experiment, and 96% are within 3σ ; these are close to the standard normal quantiles of 68% and 99% respectively, so we conclude that these theoretical uncertainties are sensible.

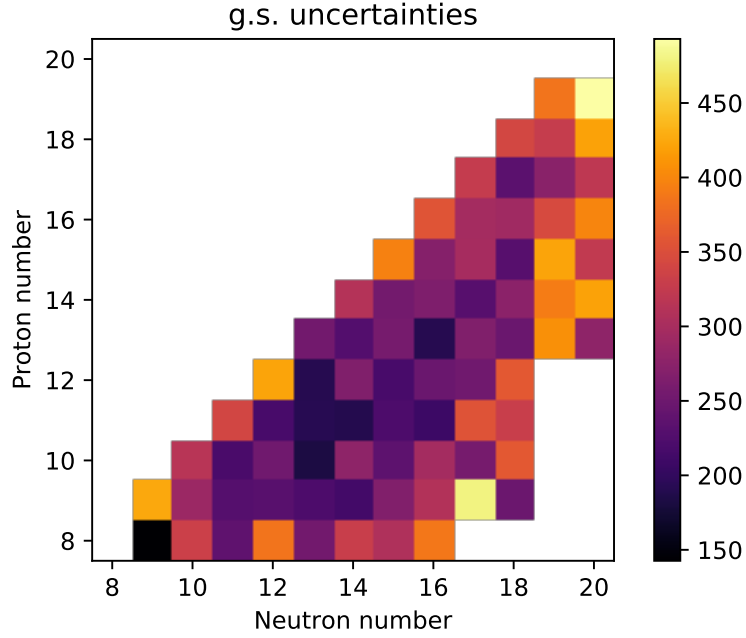


FIG. 2: Estimated 1σ uncertainties of ground-state fit energies in units of keV.

| Nucleus | J_n^π | T | $E^{exp} - E^{SM}$ (keV) | σ (keV) |
|------------------|------------|-----|--------------------------|----------------|
| ^{30}Si | 1_1^+ | 1 | -114 | 851.489 |
| ^{39}K | $1/2_1^+$ | 1/2 | -189 | 785.8 |
| ^{25}F | $5/2_1^+$ | 7/2 | -312.1 | 743.4 |
| ^{38}K | 1_1^+ | 0 | -355.9 | 686.8 |
| ^{27}Al | $11/2_1^+$ | 1/2 | -52.9 | 615.0 |
| ... | ... | ... | ... | ... |
| ^{17}O | $5/2_1^+$ | 1/2 | 218.3 | 142.6 |
| ^{23}Na | $11/2_1^+$ | 1/2 | -15.3 | 153.1 |
| ^{28}Mg | 2_1^+ | 2 | 19.3 | 153.1 |
| ^{20}Ne | 6_1^+ | 0 | -223.2 | 154.2 |
| ^{24}Mg | 6_1^+ | 0 | 156.1 | 156.4 |

TABLE II: States in experimental energy data, shown in order of descending uncertainty σ (high-variability on top, low-variability on bottom).

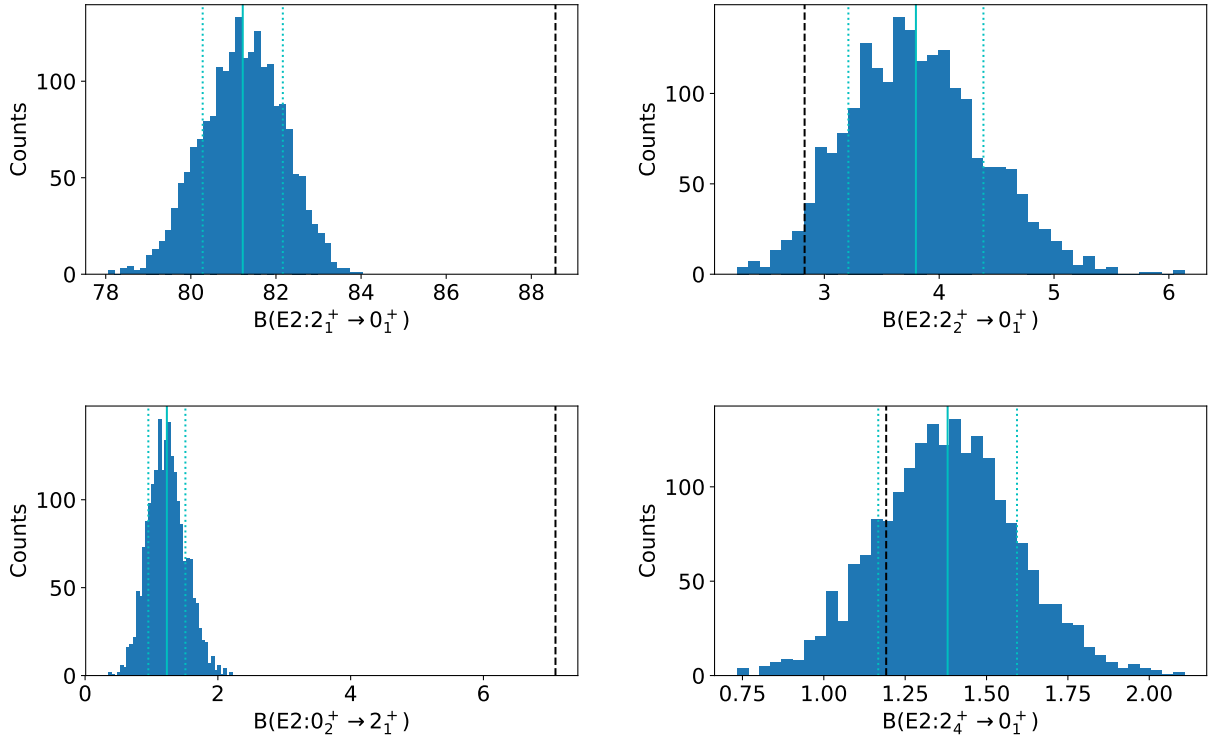


FIG. 3: Distributions of the electric quadrupole (E2) transition strengths for ^{26}Mg . Black dashed line shows experimental value [30]. The 1σ interval is highlighted in cyan.

Clockwise from top-left, $\mu \pm \sigma$ is 81.22 ± 0.94 , 3.8 ± 0.59 , 1.23 ± 0.28 , and 1.38 ± 0.21

Akin to the original error analysis of fit energies [18], Fig. 2 shows theoretical 1σ uncertainties on ground-state binding energies. We refer the reader to [29] for comparison to error plots, in particular Fig. 10 of that paper.

We also computed the uncertainties in several selected transitions. Following [26], we compute reduced transition strengths $B(E2)$ for several low-lying transitions in ^{26}Mg , shown in Fig. 3. The 1-body electric quadrupole operator matrix elements were computed assuming harmonic oscillator radial wave functions with oscillator length $b = 1.802$ [31] and effective charges $e_p = 1.57$, $e_n = 0.45$, which we obtained by a quadratic fit to experimental residuals. While some values are close to experiment, others differ significantly. The $B(E2)$ values are quadratically dependent upon both the oscillator length and the effective charges, and can be quite sensitive to small changes in the interaction matrix elements [26].

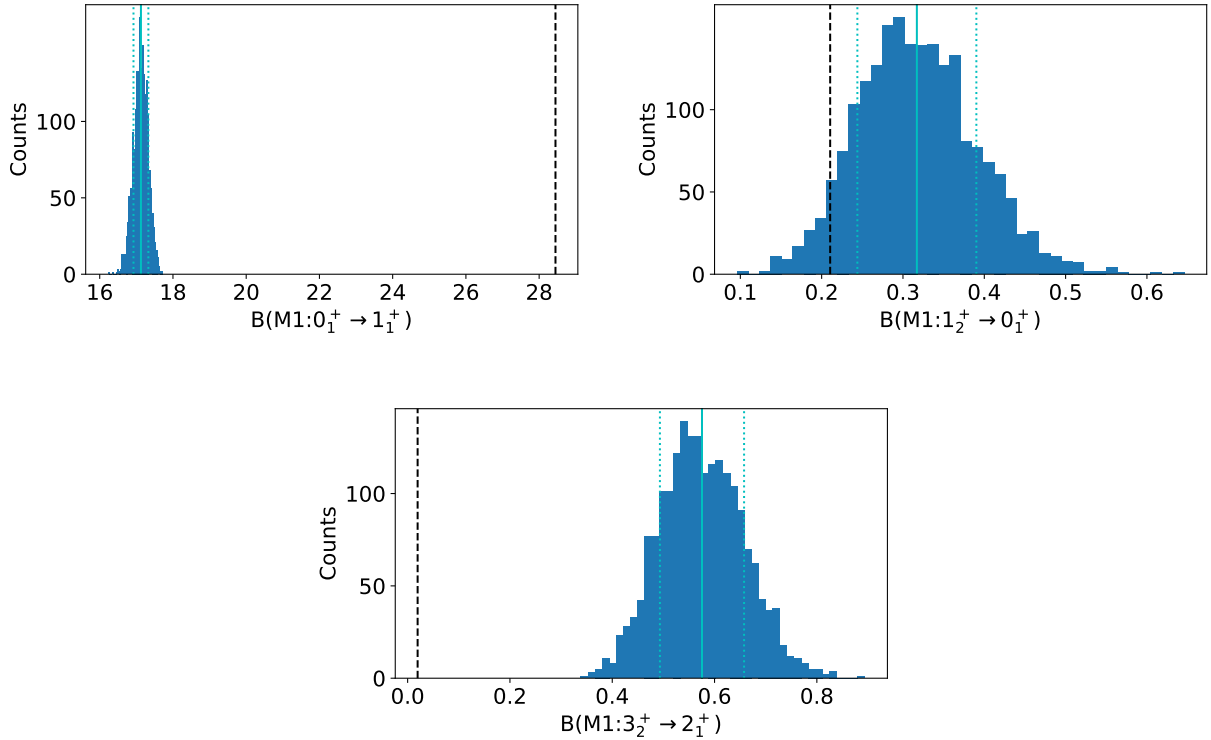


FIG. 4: Distributions of the magnetic dipole transition strengths for ^{18}F . Black dashed line shows experimental value [30]. The 1σ interval is highlighted in cyan. Clockwise from top-left, $\mu \pm \sigma$ is 17.13 ± 0.2 , 0.32 ± 0.07 , and 0.58 ± 0.08 .

Magnetic dipole reduced transition strengths $B(M1)$ distributions for ^{18}F are shown in Fig. 4. We used bare gyromagnetic factors, with no corrections for exchange currents. Like the $B(E2)$ values, some of the transitions are close to experiment, while the $0_1^+ \rightarrow 1_1^+$ is quite far away.

Finally, in Fig. 5 we show Gamow-Teller matrix elements for β^- -decays in ^{26}Ne . Here we have used for the axial-vector coupling constant $g_A/g_V = -1.27$ and a quenching factor of 0.77, following [25].

One of the biggest questions in physics today is the nature of non-baryonic dark matter [32]. While there are a number of ongoing and planned experiments [33], interpreting experiments, including limits, requires good knowledge of the dark matter-nucleus scattering cross-section, including uncertainties. While historically it was assumed dark matter would

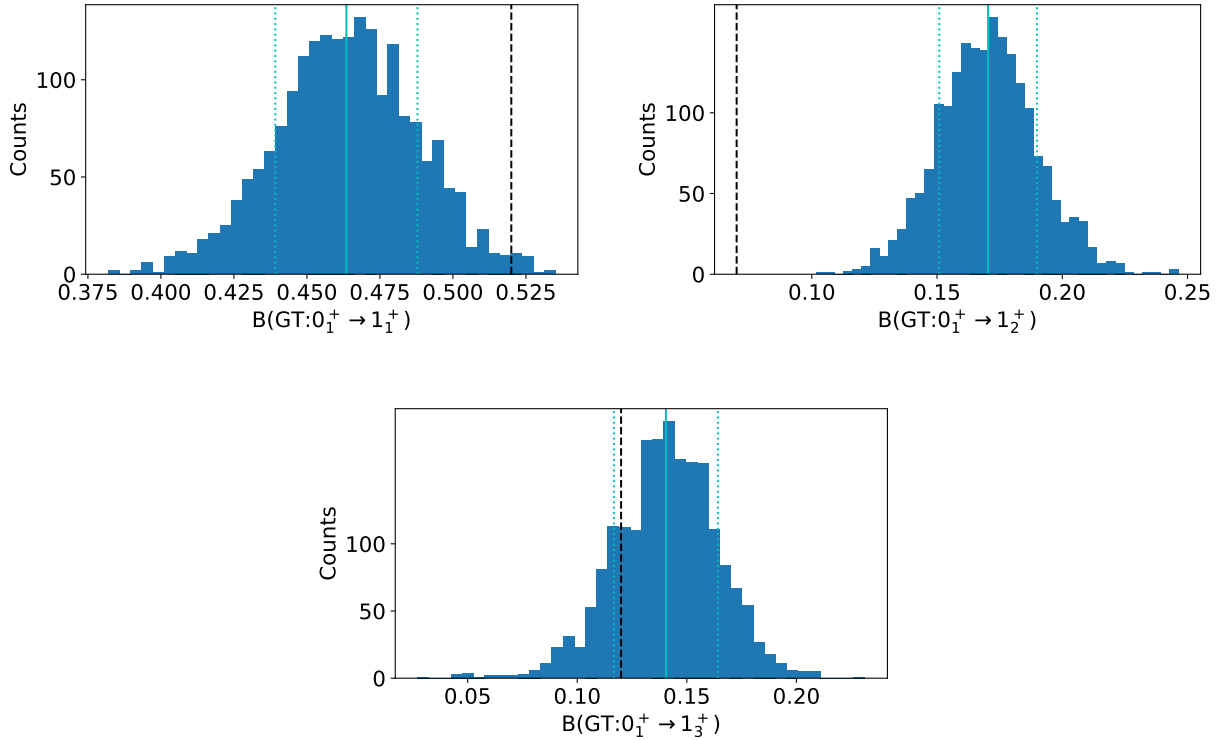


FIG. 5: Distributions of the Gamow-Teller (GT) transition strengths for ^{26}Ne . Black dashed line shows experimental value [29]. The 1σ interval is highlighted in cyan.

Clockwise from top-left, $\mu \pm \sigma$ is 0.46 ± 0.02 , 0.17 ± 0.02 , and 0.14 ± 0.02 .

couple either to the nucleon density or spin density, more recent work based upon effective field theory showed there should be a large number of low-energy couplings, around 15 [34]. This enlarged landscape of couplings, and the increased need for good theory, is a strong motivation for the current work.

In order to illustrate the application of UQ to nuclear matrix elements for dark matter scattering, Fig. 6 shows the uncertainty of an $\vec{l} \cdot \vec{s}$ coupling for ^{36}Ar . ^{36}Ar is a small component (0.3%) of argon dark matter detectors, e.g. [35], but it is within the scope of the current work to compute. Of the EFT operators that do not vanish for a $J^\pi = 0^+$ ground state, most of them depend upon radial wave functions that do not play a role in fitting the USDB parameter; one nontrivial operator, however, include $\vec{l} \cdot \vec{s}$, which arises in computing the

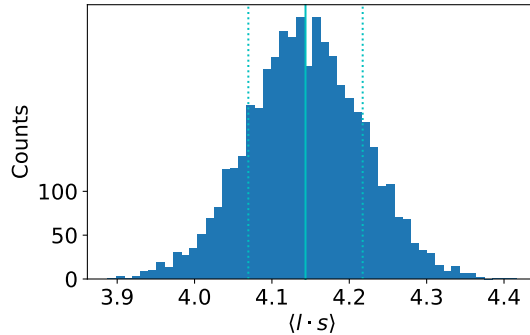


FIG. 6: Distribution of $\langle l \cdot s \rangle$ in the ground-state of ^{36}Ar . The 1σ interval is highlighted in cyan. $\mu \pm \sigma = 4.143 \pm 0.074$

nuclear matrix elements of the operators [34]

$$\begin{aligned}
 & i\vec{S}_N \cdot \left(\frac{\vec{q}}{m_N} \times \vec{v}^\perp \right), \\
 & \vec{S}_\chi \cdot \left(\vec{S}_N \times \vec{v}^\perp \right), \\
 & - \left(\vec{S}_\chi \cdot \frac{\vec{q}}{m_N} \right) \left(\left(\vec{S}_N \times \vec{v}^\perp \right) \cdot \frac{\vec{q}}{m_N} \right),
 \end{aligned}$$

where m_N is the nucleon mass, \vec{q} is the momentum transfer, $\vec{S}_{N/\chi}$ are the spins of the nucleon/WIMP, and \vec{V}^\perp is the component of the nucleon-WIMP relative velocity perpendicular to \vec{q} . We chose to study $\langle \vec{l} \cdot \vec{s} \rangle$ for the simple reason of best illustrating a variance due to uncertainty in the USDB parameters. The variance of this particular operator is relatively small, but in larger model spaces there could be greater uncertainty.

V. CONCLUSIONS

We have carried out uncertainty quantification of a ‘gold-standard’ empirical interaction for nuclear configuration-interaction calculations in the sd -shell valence. Rather than finding the uncertainty in each parameter independently [7], we computed the linear sensitivity of the energies, which is easy to compute using the Feynman-Hellmann theorem, and then constructed an approximate Hessian which we then diagonalized. This is equivalent to a singular-value decomposition of the linear sensitivity and is also known as principle com-

ponent analysis. We found evidence that this is a good approximation to the full Hessian. From the inverse of the diagonal (in a basis of the PCA linear combination of parameters) approximate Hessian, we obtained approximately independent error in the PCA parameters. Then, starting from those uncertainties, we generated uncertainties for energies as well as several observables.

In future work we will carry out a more detailed and thorough study of the Hessian, as well as applying our methods to other empirical interactions in other model spaces. For the time being, however, it seems that this approximate Hessian is a good approximation. This is not surprising, but it is useful. Nonetheless, moving to larger spaces, which grow exponentially in dimensions and compute time, will be challenging. New technologies still in development, such as quantum computing may make possible better and more rigorous uncertainty quantification.

VI. ACKNOWLEDGEMENT

We thank R. Navarro Perez for very helpful discussions on UQ. This material is based upon work supported by the U.S. Department of Energy, Office of Science, Office of Nuclear Physics, under Award Numbers DE-FG02-96ER40985 (for nuclear structure) and DE-SC0019465 (for dark matter matrix elements).

-
- [1] B. Carlsson, A. Ekström, C. Forssén, D. F. Strömberg, G. Jansen, O. Lilja, M. Lindby, B. Mattsson, and K. Wendt, *Physical Review X* **6**, 011019 (2016).
 - [2] R. N. Pérez, J. Amaro, and E. R. Arriola, *International Journal of Modern Physics E* **25**, 1641009 (2016).
 - [3] K. Wendt, B. Carlsson, and A. Ekström, arXiv preprint arXiv:1410.0646 (2014).
 - [4] A. E. Lovell, F. M. Nunes, J. Sarich, and S. M. Wild, *Phys. Rev. C* **95**, 024611 (2017).
 - [5] N. Schunck, J. D. McDonnell, D. Higdon, J. Sarich, and S. Wild, *Nuclear Data Sheets* **123**, 115 (2015).

- [6] J. D. McDonnell, N. Schunck, D. Higdon, J. Sarich, S. M. Wild, and W. Nazarewicz, *Phys. Rev. Lett.* **114**, 122501 (2015).
- [7] S. Yoshida, N. Shimizu, T. Togashi, and T. Otsuka, *Phys. Rev. C* **98**, 061301 (2018).
- [8] R. Furnstahl, D. Phillips, and S. Wesolowski, *Journal of Physics G: Nuclear and Particle Physics* **42**, 034028 (2015).
- [9] B. D. Carlsson, A. Ekström, C. Forssén, D. F. Strömberg, G. R. Jansen, O. Lilja, M. Lindby, B. A. Mattsson, and K. A. Wendt, *Phys. Rev. X* **6**, 011019 (2016).
- [10] P. Brussard and P. Glaudemans, *Shell-model applications in nuclear spectroscopy* (North-Holland Publishing Company, Amsterdam, 1977).
- [11] E. Caurier, G. Martinez-Pinedo, F. Nowacki, A. Poves, and A. P. Zuker, *Reviews of Modern Physics* **77**, 427 (2005).
- [12] B. A. Brown and B. H. Wildenthal, *Annual Review of Nuclear and Particle Science* **38**, 29 (1988).
- [13] P. Navrátil, J. Vary, and B. Barrett, *Physical Review C* **62**, 054311 (2000).
- [14] B. R. Barrett, P. Navrátil, and J. P. Vary, *Progress in Particle and Nuclear Physics* **69**, 131 (2013).
- [15] R. J. Furnstahl, S. N. More, and T. Papenbrock, *Phys. Rev. C* **89**, 044301 (2014).
- [16] G. Hagen, T. Papenbrock, D. J. Dean, and M. Hjorth-Jensen, *Physical Review C* **82**, 034330 (2010).
- [17] S. R. Stroberg, H. Hergert, S. K. Bogner, and J. D. Holt, *Annual Review of Nuclear and Particle Science* **69**, 307 (2019), <https://doi.org/10.1146/annurev-nucl-101917-021120>.
- [18] B. A. Brown and W. A. Richter, *Phys. Rev. C* **74**, 034315 (2006).
- [19] C. W. Johnson and P. G. Krastev, *Phys. Rev. C* **81**, 054303 (2010).
- [20] H. Hellman, Franz Deuticke, Leipzig , 285 (1937).
- [21] R. P. Feynman, *Phys. Rev.* **56**, 340 (1939).
- [22] C. W. Johnson, W. E. Ormand, and P. G. Krastev, *Computer Physics Communications* **184**, 2761 (2013).
- [23] C. W. Johnson, W. E. Ormand, K. S. McElvain, and H. Shan, arXiv preprint arXiv:1801.08432 (2018).

- [24] R. R. Whitehead, A. Watt, B. J. Cole, and I. Morrison, *Advances in Nuclear Physics* **9**, 123 (1977).
- [25] W. A. Richter, S. Mkhize, and B. A. Brown, *Phys. Rev. C* **78**, 064302 (2008).
- [26] W. A. Richter and B. A. Brown, *Phys. Rev. C* **80**, 034301 (2009).
- [27] D. S. Sivia and J. Skilling, *Data Analysis: A Bayesian Tutorial*, 2nd ed. (Oxford Science Publications, 2006).
- [28] While this is a popular choice of prior, there are other sensible choices. For instance, a similar study may incorporate the space of all USD interactions into an informative prior, since this set of Hamiltonians informs the possible parameter distributions.
- [29] L. Weissman, O. Arndt, U. Bergmann, J. Cederkall, I. Dillmann, O. Hallmann, L. Fraile, S. Franchoo, L. Gaudefroy, U. Köster, K. L. Kratz, A. F. Lisetskiy, B. Pfeiffer, O. Sorlin, and S. Tabor, *Phys. Rev. C* **70**, 057306 (2004).
- [30] M. Wang, G. Audi, A. H. Wapstra, F. G. Kondev, M. MacCormick, X. Xu, and B. Pfeiffer, *Chin.Phys.C* **36**, 1603 (2012).
- [31] B. A. Brown and B. Wildenthal, *Annual Review of Nuclear and Particle Science* **38**, 29 (1988).
- [32] G. Bertone and D. Hooper, *Rev. Mod. Phys.* **90**, 045002 (2018).
- [33] L. Roszkowski, E. M. Sessolo, and S. Trojanowski, *Reports on Progress in Physics* **81**, 066201 (2018).
- [34] N. Anand, A. L. Fitzpatrick, and W. C. Haxton, *Phys. Rev. C* **89**, 065501 (2014).
- [35] P. Agnes, T. Alexander, A. Alton, K. Arisaka, H. Back, B. Baldin, K. Biery, G. Bonfini, M. Bossa, A. Brigatti, *et al.*, *Physics Letters B* **743**, 456 (2015).